

Certain BCS wavefunctions are quantum many-body scars

Kiryl Pakrouski¹, Zimo Sun,²

¹*Institute for Theoretical Physics, ETH Zurich, 8093 Zurich, Switzerland and*

²*Department of Physics, Princeton University, Princeton, NJ 08544, USA*

(Dated: November 22, 2024)

We provide a method for constructing many-body scar states in fermionic lattice models that incorporate a given type of correlations with one of the states maximizing them over the full Hilbert space. Therefore this state may always be made the ground state by adding such correlations as a "pairing potential" δH_0 to any Hamiltonian $H = H_0 + OT$ supporting group-invariant scars [1]. In case of single-flavour spin-full fermions the ground state is a special case of the BCS wavefunction written in real space and invariant under any site index relabelling. For multi-orbital fermions this state also resembles BCS but includes higher order terms corresponding to "pairing" of more than two fermions. The broad class of eligible Hamiltonians H is well documented [1, 2] and includes many conventional condensed matter interactions. The part of the Hamiltonian ($H_0 + \delta H_0$) that governs the exact dynamics of the scar subspace coincides with the BCS mean-field Hamiltonian. We therefore show that its BCS ground state and the excitations above it are many-body scars that are dynamically decoupled from the rest of the Hilbert space and thereby protected from thermalization. These states are insensitive to a variety of OT Hamiltonian terms that among others include interactions and (spin-orbit) hoppings. Our results point out a connection between the fields of superconductivity and weak ergodicity breaking (many-body scars) and will hopefully encourage further investigations. They also provide the first practical protocol to initialize a fermionic system to a scar state in (a quantum simulator) experiment.

I. INTRODUCTION

Superconductivity [3] is one of the best-understood quantum condensed matter phenomena and yet is the one that still conceals some of the most intriguing secrets such as the mechanisms underlying unconventional superconductivity.

As a macroscopic quantum phenomenon, superconductivity reflects the collective behaviour of many degrees of freedom. The emergence of statistical physics from individual quantum eigenstates can be analyzed in terms of eigenstate thermalization hypothesis (ETH) that conjectures that a macroscopic thermal average of an observable should agree with any measurements made in individual eigenstates at the corresponding temperature/energy.

Many-body scars are eigenstates of strongly-interacting Hamiltonians that elude this description [4–8] by weakly breaking ergodicity. They are found in a variety of systems [1, 2, 9–53] and may be understood within several frameworks [1, 10, 54]. We will base our discussion on Ref. [1] and think about scars as a subspace that dynamically decouples from the rest of the Hilbert space and is governed by often simple and integrable Hamiltonian H_0 while the Hamiltonian of the full system $H = H_0 + OT$ is strongly interacting and has almost no symmetries. For certain simple H_0 the time evolution within the scar subspace follows "closed orbits" which manifests as "revivals" in experiments [4].

One way to discuss superconductivity is using the concept of the off-diagonal long-range order (ODLRO), the presence of non-decaying with distance two-point correlations between pair annihilation and creation operators at distant sites [55]. These correlations or eta pairing can

also be used as an indicator of superconductivity induced by some kind of external drive in pump-probe experiments [56–58]. The concept of ODLRO was introduced by Yang who also constructed the eta-pairing states [59] (see [60] for a generalization), eigenstates of the Hubbard model that possess ODLRO [59, 61].

Interestingly, exactly these states have recently been found to be many-body scars [19, 23] relevant to several important concepts such as spectrum-generating algebras [27, 29] which in turn are relevant in a broader context of open quantum systems [18].

Could this coincidence hint that the phenomena of many-body scars and superconductivity are related? Ref [62] recently provided another hint supporting this idea by constructing analogues of eta pairing states with unconventional types of pairing albeit in a somewhat artificial fine-tuned model with multi-body interactions.

One could at first see a contradiction in the fact that the analysis of superconductivity usually starts from the ground state whereas the many-body scars are typically scattered around the spectrum. Further, the eta-pairing states have fixed particle number and therefore the expectation value of a pair creation operator in such a state is zero.

In an attempt to make a scar the ground state we add $\delta H_0 = -(\mathcal{O}^\dagger + \mathcal{O})$ to a Hamiltonian that is known to support scars, where \mathcal{O}^\dagger is a pair creation operator. Eta pairing states are known [1, 59, 63] to have large ODLRO $\langle \mathcal{O}_i^\dagger \mathcal{O}_j \rangle$ and one could thus hope that they are susceptible to δH_0 and would move towards low energy. Remarkably, we find that not only a state from a scar subspace becomes the ground state but it also happens to be the BCS wavefunction! δH_0 therefore "rotated" the eta pairing states to form linear combinations with indefinite to-

tal particle number thereby removing the second obstacle mentioned above.

In this work, we first present a general solution explaining the above observations for two types ("superconducting" and "magnetic") of rather general bilinear fermionic excitation operators \mathcal{O}^\dagger . This solution involves a BCS-like wavefunction that in multi-orbital systems includes terms $(\mathcal{O}^\dagger)^m$ with $m > 1$. The BCS ground state and its excitations are shown to be many-body scars for a broad class of fermionic lattice Hamiltonians. We discuss two examples. In the single-orbital case we consider two superconducting (both eta-pairing) and one magnetic \mathcal{O}^\dagger . In the two-orbital case we consider an "inter-band", magnetic \mathcal{O}^\dagger and illustrate the presence of the $(\mathcal{O}^\dagger)^2$ contribution in the BCS-like ground state. In both cases the model is a deformed Hubbard Hamiltonian.

δH_0 can be thought of as a BCS mean-field Hamiltonian and we comment on the extra stability its solution has due to the fact that it is also a scar. Our findings strengthen the case that many-body scars may be related to superconductivity and provide a lead to further exploration in this direction.

II. GENERAL CASE

A. The two types of excitations

We will consider two types of local excitations in fermionic systems which have slightly different requirements to the Hilbert space.

For the excitations of type I we consider the Hilbert space of complex fermions $\{c_{i\alpha}^\dagger, c_{j\beta}\} = \delta_{\alpha\beta}\delta_{ij}$, where $1 \leq i, j \leq N$ are site indexes on an arbitrary lattice of arbitrary dimension and $1 \leq \alpha, \beta \leq 2K$ are the "flavour" indexes that may simply be spin or also include further degrees of freedom such as layer or orbital.

Let A be a $2K \times 2K$ antisymmetric and unitary matrix. These two conditions can be satisfied only when $2K$ is even because $A^T = -A$ implies $\det A = 0$ for odd $2K$ which would contradict $A^\dagger A = 1$.

At each site j , define a fermion bilinear of type I

$$\mathcal{O}_j = \frac{1}{2} \sum_{\alpha, \beta=1}^{2K} c_{j\alpha} A_{\alpha\beta} c_{j\beta} . \quad (\text{II.1})$$

which gives

$$[\mathcal{O}_j, \mathcal{O}_j^\dagger] = K - n_j, \quad (\text{II.2})$$

where n_j is the particle number operator at site j .

Creating excitations of type I (II.1) changes the particle number and therefore the natural "vacuum" for this type of excitations coincides with standard vacuum

$$|0_I\rangle = |0\rangle \quad (\text{II.3})$$

the state without any fermions.

For the excitations of type II we consider the Hilbert space of spin- $\frac{1}{2}$ fermions that can have an additional flavour index α , satisfying the standard anticommutation relations $\{c_{i\alpha\sigma}^\dagger, c_{j\beta\sigma'}\} = \delta_{\alpha\beta}\delta_{\sigma\sigma'}\delta_{ij}$, where i, j are site labels and $\sigma, \sigma' \in \{\uparrow, \downarrow\}$ are spin indices. The fermion bilinear of type II is defined as

$$\mathcal{O}_j = \sum_{\alpha=1}^K c_{j\alpha\downarrow}^\dagger \tilde{A}_{\alpha\beta} c_{j\beta\uparrow} \quad (\text{II.4})$$

where $\tilde{A}_{\alpha\beta}$ is a $K \times K$ unitary matrix, i.e. $\tilde{A}^\dagger \tilde{A} = 1$.

The commutator

$$[\mathcal{O}_j, \mathcal{O}_j^\dagger] = -M_j \quad (\text{II.5})$$

where $M_j = n_{j\uparrow} - n_{j\downarrow}$ is the magnetization at site j .

The excitations of type II are "magnetic" and the natural vacuum in this case is a half-filled state with all spins down

$$|0_{II}\rangle = c_{j1\downarrow}^\dagger \cdots c_{jK\downarrow}^\dagger |0\rangle \quad (\text{II.6})$$

For both types the operators $\mathcal{O}_j, \mathcal{O}_j^\dagger$ and their commutator generate an $SU(2)$ algebra and we can make the following identifications

$$J_+^{(j)} \Leftrightarrow \mathcal{O}_j, \quad J_-^{(j)} \Leftrightarrow \mathcal{O}_j^\dagger, \quad J_3^{(j)} \Leftrightarrow \frac{1}{2}[\mathcal{O}_j, \mathcal{O}_j^\dagger]. \quad (\text{II.7})$$

For two specific choices of matrix A and single-flavour case this observation was made in Ref. [61] and the two $SU(2)$ groups were identified as spin and pseudo-spin.

For both excitation types the maximum value of $J_3^{(j)}$ (and therefore of $J_1^{(j)}$ and $J_2^{(j)}$) is limited by $K/2$ from which we conclude that the largest representation we can have is of "spin" $K/2$ meaning the operator \mathcal{O}_j^\dagger can be applied the maximum of K times to its respective on-site vacuum before producing a 0. Therefore the maximum number of on-site excitations of either type is K .

Note that i and j could also be k_i and k_j - indexes of the points in the momentum space. All the results we obtain in this work would apply if we made that substitution throughout, including all the Hamiltonian terms.

B. The $O(N)$ -invariant many-body scars

Matrices $A_{\alpha\beta}$ and $\tilde{A}_{\alpha\beta}$ do not depend on the site j thus summing over all sites we obtain an $O(N)$ -symmetric operator

$$\mathcal{O} = \sum_j \mathcal{O}_j, \quad (\text{II.8})$$

where the $O(N)$ group acts on the site label of c and c^\dagger and $O(N)$ -invariance can be thought of as independence on any relabelling of sites.

Let $|0_\phi\rangle$ be a state that is $O(N)$ -invariant, has no excitations of type \mathcal{O}_j^\dagger and is a zero-eigenvalue eigenvector of \mathcal{O} thus satisfying $\langle 0_\phi | \mathcal{O} | 0_\phi \rangle = 0$. Depending on the excitation type the states $|0_I\rangle$ and $|0_{II}\rangle$ satisfy this requirement.

Consider the wavefunctions

$$|\phi_n\rangle = \frac{(\sum_i \mathcal{O}_i^\dagger)^n |0_\phi\rangle}{P_N(n)}, \quad 0 \leq n \leq NK, \quad (\text{II.9})$$

where $P_N(n) = \sqrt{\frac{(NK)!n!}{(NK-n)!}}$.

The wavefunctions $|\phi_n\rangle$ by construction have symmetry $O(N)$ as a result of $O(N)$ -symmetric operator acting on an $O(N)$ -symmetric state $|0_\phi\rangle$. The full symmetry G of these states, depending on a particular \mathcal{O}_j^\dagger and particular Hilbert space may be higher and would then contain $O(N)$ as a sub-group. Because the operator (II.4) conserves particle number any type-II states will always be at half-filling just as the $|0_{II}\rangle$ is.

The wavefunctions (II.9) are constructed by explicitly building in \mathcal{O}_i^\dagger correlations. Therefore the subspace spanned by them can be expected to have high expectation values $\langle \mathcal{O}_i^\dagger \rangle$, $\langle \mathcal{O}_i^\dagger \mathcal{O}_j \rangle$ and also high "susceptibility" to the term \mathcal{O}_i^\dagger added to the Hamiltonian.

Because the subspace (II.9) is $O(N)$ -invariant any state from that subspace is a group-invariant many-body scar [1] for any Hamiltonian of the form

$$H = H_0 + OT, \quad (\text{II.10})$$

where O is an arbitrary operator, T is a generator of G . H_0 has to satisfy $[H_0, C_G^2] = W_c \cdot C_G^2$, where W_c is some operator and C_G^2 is the quadratic Casimir of the group G . In particular, this condition is satisfied by an H_0 that is G -invariant. G is a continuous group that is $O(N)$ or that contains $O(N)$ as a sub-group. Various Hamiltonian terms that can be used as H_0 or T for single-band fermionic Hilbert space have been discussed in Ref. [2] and the ones suitable for multi-flavour fermions in Ref. [64].

Note that any OT term annihilates any state in (II.9) exactly and the spectrum within that $NK + 1$ -dimensional subspace is determined solely by H_0 .

In the Appendix B we argue that almost any admissible bilinear H_0 term is a linear combination of the three $SU(2)$ generators $[\mathcal{O}_j, \mathcal{O}_j^\dagger; \mathcal{O}_j; \mathcal{O}_j^\dagger]$. The only restriction is that for type-I all the chemical potentials terms μn_α must have flavour-independent strength μ . Similarly, for type-II we have to require that all the couplings B in the terms of the form $B(n_{\alpha\uparrow} - n_{\alpha\downarrow})$ are also flavour-independent.

This motivates us to consider H_0 parametrised as

$$H_0 = - \sum_j \mu [\mathcal{O}_j, \mathcal{O}_j^\dagger] + \delta H_0 + C, \quad (\text{II.11})$$

$$\delta H_0 = -\gamma e^{-i\theta} \mathcal{O}_j - \gamma e^{i\theta} \mathcal{O}_j^\dagger \quad (\text{II.12})$$

where C , μ , γ and θ are real numbers. For type I μ plays the role of the chemical potential while for type II of the z magnetic field.

Within the scar subspace spanned by (II.9) the Hamiltonian H_0 and the full Hamiltonian H are given by a $(NK + 1) \times (NK + 1)$ tri-diagonal matrix with diagonal matrix elements determined by μ and the off-diagonal ones given by $H_{n,n+1} = \gamma e^{i\theta} \frac{P_N(n)}{P_N(n-1)} = \gamma e^{i\theta} \sqrt{(NK - n + 1)n}$.

For any type-I \mathcal{O} the Hamiltonian H_0 (II.11) coincides with the BCS mean-field Hamiltonian written down in real space. Further, the interactions such as Hubbard are typically [2] in the OT part of the Hamiltonian. Therefore the mean field Hamiltonian H_0 typically thought of as an approximation to an interacting problem is actually the exact Hamiltonian of strongly-interacting electrons within the scar subspace!

We now proceed to solve H_0 which fully determines the dynamics within the scar subspace as long as the full Hamiltonian is of the form (II.10).

C. Solution for H_0

Summing the local $SU(2)$ generators (II.7) over all sites $J_a \equiv \sum_j J_a^{(j)}$ we obtain a global $SU(2)_A$ (subscript indicates the matrix that induces the group) algebra acting on the full Hilbert space. Because of this action, the Hilbert space decomposes into irreducible representations of $SU(2)_A$. The largest representation in this decomposition has dimension $NK + 1$ and the corresponding lowest weight state is simply the type-I or type-II vacuum.

Observing that the coefficients in (II.11) are site-independent and using the identification (II.7) and the commutation relations (II.2) and (II.5), we can rewrite H_0 as

$$H_0 = C + 2\sqrt{\gamma^2 + \mu^2} \left(-\frac{e^{-i\theta} J_+ + e^{i\theta} J_-}{2 \cosh \tau} + \tanh \tau J_3 \right), \quad (\text{II.13})$$

where $\sinh \tau \equiv -\frac{\mu}{\gamma}$ and $C = \mu KN$ for type I or $C = 0$ for type II.

We now recall some basic results from the representation theory of an $SU(2)$ group with generators J_1, J_2, J_3 . Consider a dimension $2h + 1$ irreducible representation of $SU(2)$. A basis that diagonalizes J_3 is $|n\rangle$, i.e. $J_3 |n\rangle = n |n\rangle$, where $n = -h, -h + 1, \dots, h - 1, h$. In terms of this basis, the largest eigenvalue of J_1 corresponds to the coherent state $e^{J_-} |h\rangle$, where $J_\pm = J_1 \pm iJ_2$. More generally, for any $z \equiv e^{\tau + i\theta} \in \mathbb{C}$, define (unnormalized) coherent states

$$|z\rangle \equiv e^{zJ_-} |h\rangle, \quad (\text{II.14})$$

satisfying the inner product

$$\langle \bar{w} | z \rangle = (1 + \bar{w}z)^{2h}, \quad \bar{w} \equiv w^*. \quad (\text{II.15})$$

The action of the SU(2) algebra on these coherent states is given by

$$\begin{aligned} J_+|z\rangle &= (2hz - z^2\partial_z)|z\rangle, & J_-|z\rangle &= \partial_z|z\rangle, \\ J_3|z\rangle &= (h - z\partial_z)|z\rangle. \end{aligned} \quad (\text{II.16})$$

For any fixed z , the state $|z\rangle$ is the (lowest) eigenvalue $-h$ eigenstate of the following Hamiltonian

$$H_z = -\frac{e^{-i\theta}J_+ + e^{i\theta}J_-}{2\cosh\tau} + \tanh\tau J_3. \quad (\text{II.17})$$

This particular linear combination of the SU(2) generators is found by first imposing the cancellation of the ∂_z terms and then tuning the overall normalization such that it is equal to $-h$. The full spectrum of H_z is the same as that of J_3 : $E_n = n \in \{-h, -h+1, \dots, h-1, h\}$.

The remaining eigenstates can be generated by acting on $|z\rangle$ with

$$O^{\gamma\dagger} = \frac{\bar{z}J_+ - \bar{z}^{-1}J_-}{2\cosh\tau} + \frac{J_3}{\cosh\tau}, \quad (\text{II.18})$$

where the pre-factor is chosen such that the operator $O^{\gamma\dagger}$ is related to J_+ by a SU(2) rotation and is thus a normalized raising operator in the new "rotated" tower.

At this point we can already compute the 1-point expectation value in the coherent state

$$\langle z|J_-^j|z\rangle = \frac{K e^{-i\theta}}{2\cosh\tau} \quad (\text{II.19})$$

Comparing our Hamiltonian (II.13) with the general form (II.17) and identifying $|h\rangle = |0_I\rangle$ or $|h\rangle = |0_{II}\rangle$ we write down the solution for (II.13) with the ground state energy

$$E_0 = C - KN\sqrt{\gamma^2 + \mu^2} \quad (\text{II.20})$$

and the corresponding product state wavefunction

$$|\psi_0\rangle = N_\psi \prod_j e^{\frac{v}{u}\mathcal{O}_j^\dagger} |0_\phi\rangle, \quad N_\psi = u^{NK}, \quad (\text{II.21})$$

where

$$\begin{aligned} u &= \sqrt{\frac{1+X}{2}}, & v &= e^{i\theta} \sqrt{\frac{1-X}{2}}, \\ X &= \frac{\mu}{E}, & E &= \sqrt{\gamma^2 + \mu^2}. \end{aligned} \quad (\text{II.22})$$

The normalization factor N_ψ follows from the inner product (II.15).

For the Hilbert space of single-orbital spin-1/2 fermions the wavefunction (II.21) coincides (see also Sec. III) with the BCS wavefunction [3] where its coefficients u and v are independent of the position on the lattice. This space-invariance is a consequence of the $O(N)$ invariance of $|\psi_0\rangle$, the NK excited states above it and of the original basis (II.9) for this subspace we started from.

Furthermore, all these states are many-body scars for a broad class of Hamiltonians (II.10).

For multi-flavour fermions with $K \geq 2$ the expansion in the wavefunction (II.21) contains higher (up to K) powers of \mathcal{O}_j^\dagger

$$|\psi_0\rangle = N_\psi \prod_j \left(1 + \frac{v}{u}\mathcal{O}_j^\dagger + \frac{(\frac{v}{u}\mathcal{O}_j^\dagger)^2}{2} + \dots + \frac{(\frac{v}{u}\mathcal{O}_j^\dagger)^K}{K!} \right) |0_\phi\rangle. \quad (\text{II.23})$$

The power- m terms $(\mathcal{O}_j^\dagger)^m$ may be interpreted as clustering together of $2m$ fermions by analogy with pairing for $m = 1$. We expect that the relative magnitude of the correlations of different order m is controlled by the ratio $\frac{v}{u}$. Namely, higher- m clustering dominates for $\frac{v}{u} > 1$ which corresponds to $\mu < 0$ for $\theta = 0$ while regular pairing dominates for $\mu > 0$.

The spectrum of (II.17) is equidistant with the energy gap of 1. With the pre-factor in (II.13) the spectrum in our case is

$$E_n = E_0 + n2E; \quad n = 0 : 1 : NK. \quad (\text{II.24})$$

The raising operator $O^{\gamma\dagger}$ (II.18) is an analog of \mathcal{O}^\dagger : if we replace \mathcal{O}^\dagger with $O^{\gamma\dagger}$ in eq. (II.9) the resulting states $|\phi_n^\gamma\rangle$ form the full basis for the same scar subspace. Because they are equidistant in energy any initial state that is a linear superposition of $|\phi_n^\gamma\rangle$ will return to itself in time evolution with the revivals period of $\frac{2\pi}{2E} = \frac{\pi}{\sqrt{\gamma^2 + \mu^2}}$ [1] for any Hamiltonian (II.10) independently of the OT terms.

The expectation value of the operator $[\mathcal{O}, \mathcal{O}^\dagger]$ (total particle number for type-I and total z magnetization for type-II) in the $|\phi_n^\gamma\rangle$ states depends on μ .

For $\mu = 0$ they are all half-filled/zero magnetization and the highest state in the tower can be obtained by flipping the sign under the exponent in (II.21).

In Appendix A1 and A2 we demonstrate that some parts of the solution obtained here could also be derived for any fixed definition of the \mathcal{O} operator using a canonical Bogoliubov transformation. For the spin-full type-I excitations it is convenient to use the spinor notation that (similar to the Nambu spinor [65]) combines particles and holes

$$\left(c_{j1\uparrow}^\dagger \dots c_{jK\uparrow}^\dagger c_{j1\downarrow} \dots c_{jK\downarrow} \right) \quad (\text{II.25})$$

whereas for type-II the spinor that combines the "magnetic particles" (spin-up) with "holes" (spin-down)

$$\left(c_{j1\uparrow}^\dagger \dots c_{jK\uparrow}^\dagger c_{j1\downarrow}^\dagger \dots c_{jK\downarrow}^\dagger \right) \quad (\text{II.26})$$

The emergence of these two spinors can also be motivated as a more natural way to discuss the spin- and pseudo-spin SU(2) groups [66].

The raising operator $O^{\gamma\dagger}$ (II.18) in this language is constructed according to (II.1) or (II.4) where the original fermionic operators are replaced with the Bogoliubov-transformed ones.

D. Correlations and the global energy minimum

Due to the $O(N)$ invariance of $|\psi_0\rangle$ (II.21) and of any other state from the scar subspace spanned by $|\phi_n\rangle$ (II.9) the one-point functions $\langle \mathcal{O}_j^\dagger \rangle$ and $\langle \mathcal{O}_j \rangle$ do not depend on the measurement point j [1] and the two-point function $\langle \mathcal{O}_i^\dagger \mathcal{O}_j \rangle$ measured in such a state does not depend on the distance between the two points i and j . The latter property by definition [59] means that these $O(N)$ -symmetric states have the off-diagonal long-range order of type \mathcal{O}_j^\dagger .

As we argued in Sec II A the on-site $SU(2)$ formed by the operators \mathcal{O}_j and \mathcal{O}_j^\dagger has the largest representation with spin $K/2$ leading to the maximum value of $K/2$ for any of the three generators J_α measured in any state in the Hilbert space.

Therefore we have

$$\mathcal{O}_j + \mathcal{O}_j^\dagger = J_+^j + J_-^j = 2J_x^j \leq K \quad (\text{II.27})$$

A consequence of this is the bound (over all states in Hilbert space) on the value of the 1-point function

$$\text{Re}[\langle \mathcal{O}_j^\dagger \rangle] = \frac{1}{2} \langle \mathcal{O}_j + \mathcal{O}_j^\dagger \rangle = \frac{K}{2} \quad (\text{II.28})$$

As follows from (II.19) the value of the 1-point function in the ground state $|\psi_0\rangle$ (II.21) for $K = 1$ is

$$\langle \psi_0 | \mathcal{O}_j^\dagger | \psi_0 \rangle_{(K=1)} = \frac{e^{-i\theta}}{2} \sqrt{1 - X^2} = \frac{e^{-i\theta}}{2} \frac{\gamma}{\sqrt{\gamma^2 + \mu^2}} \quad (\text{II.29})$$

and decreases monotonically with μ . For $K = 2$ the one-point function is factor of two larger: $\langle \psi_0 | \mathcal{O}_j^\dagger | \psi_0 \rangle_{(K=2)} = 2 \langle \psi_0 | \mathcal{O}_j^\dagger | \psi_0 \rangle_{(K=1)}$.

The bound for the two-point function in any product state is

$$\langle \mathcal{O}_i^\dagger \mathcal{O}_j \rangle = \langle \mathcal{O}_i^\dagger \rangle \langle \mathcal{O}_j \rangle \leq \frac{K^2}{4}. \quad (\text{II.30})$$

The two bounds (II.28) and (II.30) are exactly saturated by the state $|\psi_0\rangle$ when $\mu = 0$ for any system size N (there is no N -dependence in either the bounds (II.28), (II.30) or the expectation values (II.29))!

This means that for any Hamiltonian of the form (II.10), independently of the terms that appear in OT and their strengths there exists a large enough γ_c such that the scar state $|\psi_0\rangle$ (II.23) becomes the ground state for $\mu = 0$.

For finite μ the value $\langle \psi_0 | \mathcal{O}_j^\dagger | \psi_0 \rangle$ is slowly decreasing. Numerically we observe that also at finite μ up to very large magnitudes the value of the one-point function in $|\psi_0\rangle$ is still larger than in any other state in the Hilbert space. It is however unlikely that one could guarantee this analytically due to the lack of information about the behaviour of generic states.

As long as the Hamiltonian is of the scar-preserving form (II.10) the $(NK + 1)$ -dimensional, G -invariant subspace remains dynamically decoupled from the rest of the Hilbert space. Eigenvectors and energies within the subspace are determined by H_0 . Therefore any modifications of the OT part of the Hamiltonian may only change the threshold value $|\gamma_c|$ above which a state from the subspace becomes the ground state.

III. EXAMPLE 1: 2D SINGLE-ORBITAL HUBBARD MODEL

For our first example consider the Hilbert space of spin-1/2 fermions without any additional flavours ($K=1$ for both types) on a 2D square lattice.

The starting point is the standard Hubbard Hamiltonian

$$H^H = \mu_H \sum_{i=1}^N (n_{i\uparrow} + n_{i\downarrow}) + \sum_{\langle kj \rangle} (t_{kj} c_{j\uparrow}^\dagger c_k + h.c.) + U \sum_j n_{j\downarrow} n_{j\uparrow}. \quad (\text{III.1})$$

A. Scars and $H_0 + OT$ decomposition

There are three families of scar states in this model [1, 2] for purely imaginary ($|n^\eta\rangle$), purely real ($|n^\eta\rangle'$) or complex ($|n^\zeta\rangle$) hopping amplitude t_{kj} . Each of the three families is constructed according to (II.9) where the operator \mathcal{O}_j^\dagger is given by

$$\begin{aligned} \eta_j^\dagger &= \frac{1}{2} \left(c_{j\uparrow}^\dagger c_{j\downarrow}^\dagger - c_{j\downarrow}^\dagger c_{j\uparrow}^\dagger \right) \\ \eta_j^{\prime\dagger} &= \frac{1}{2} e^{i\pi j} \left(c_{j\uparrow}^\dagger c_{j\downarrow}^\dagger - c_{j\downarrow}^\dagger c_{j\uparrow}^\dagger \right) \\ \zeta_j^\dagger &= c_{j\uparrow}^\dagger c_{j\downarrow}. \end{aligned} \quad (\text{III.2})$$

Observe that the excitations are of type-I in the first two cases and of type-II for the third case.

As shown in Ref. [2] the $H_0 + OT$ decomposition of the Hubbard model for the eta and eta' states reads

$$H^H = H_0^{H\eta} + t \sum_{\langle i,j \rangle} T'_{\langle i,j \rangle} - \frac{U}{2} \sum_i M_i^2, \quad (\text{III.3})$$

where

$$H_0^{H\eta} = n \left(\frac{U}{2} + \mu_H \right) \quad (\text{III.4})$$

with n total particle number and the remaining (OT) terms exactly annihilate any state in the scar subspaces spanned by $|n^\eta\rangle$ and $|n^\eta\rangle'$.

The decomposition for the zeta states is

$$H^H = H_0^{H\zeta} + t \sum_{\langle i,j \rangle} T'_{\langle i,j \rangle} + \frac{U}{2} \sum_i (n_i - 1)^2, \quad (\text{III.5})$$

where

$$H_0^{H\zeta} = n \left(\frac{U}{2} + \mu_H \right) - U \frac{N}{2} \quad (\text{III.6})$$

and the remaining (OT) terms annihilate any state in the zeta scar subspace spanned by $|n^\zeta\rangle$. All the zeta states are half-filled [2], therefore the action of (III.6) within the zeta subspace is just a constant $\mu_H N$.

As announced in the general discussion the scar subspace constructed using (II.9) may have symmetry G that is higher than $O(N)$. For example the $|n^\eta\rangle$ built using η^\dagger (III.2) are in addition spin-singlets and their full symmetry is $G = \widetilde{Sp}(N)$ [67]. In all three cases $O(N)$ is a sub-group of the full symmetry G .

B. BCS ground state for type-I η and η'

Now on top of the Hubbard Hamiltonian we add the pairing potential δH_0 (II.12) with \mathcal{O} from (III.2). For η and η' one can think of the resulting Hamiltonian as being a model for a Hubbard material being brought in close proximity of a superconductor. In all the three cases this additional term respects the full symmetry of the respective scar family and becomes part of H_0 . The exact full Hamiltonian that governs eta (for example) scar subspace is then

$$H_0^\eta = H_0^{H\eta} + \delta H_0^\eta \quad (\text{III.7})$$

On the other hand one could start from H_0^η (which is identical to the mean-field Hamiltonian) and consider Hubbard and any further OT terms as a perturbation that, independent of its strength, leaves the mean-field solution intact because it is a scar state.

Consider the two cases 1) real hopping in (III.1), $\mathcal{O}_j = \eta'_j$, the tower of states $|\phi_n\rangle$ (II.9) is then known as momentum $k = \pi$ eta-pairing states [59] defined on any bi-partite lattice 2) imaginary hopping in (III.1), $\mathcal{O}_j = \eta_j$, states $|\phi_n\rangle$ are then $k = 0$ eta-pairing states [1, 59] defined on arbitrary lattice). Define $s_j = e^{ikj}$.

H_0^η is of the general form (II.11) with $\mu = \frac{U}{2} + \mu_H$ and $C = (\frac{U}{2} + \mu_H)N$.

According to the general argument for a large enough γ the ground state of the Hamiltonian $H^H + \delta H_0$ is a many-body scar state

$$|\psi_0^\eta\rangle = N_\psi \prod_j \left(1 + \frac{e^{i\theta}}{\frac{\mu}{\gamma} + \sqrt{\frac{\mu^2}{\gamma^2} + 1}} s_j c_{j\uparrow}^\dagger c_{j\downarrow}^\dagger \right) |0\rangle. \quad (\text{III.8})$$

which is also the BCS wavefunction written in real space. For $\mu_H = -\frac{U}{2}$ and $\theta = 0$ it maximizes over the Hilbert space the value of the one point function $\langle s_j c_{j\uparrow}^\dagger c_{j\downarrow}^\dagger \rangle = \frac{e^{-i\theta}}{2} \frac{1}{\sqrt{1 + (\frac{U/2 + \mu_H}{\gamma})^2}}$ and its two-point function

tion $\langle \frac{s_j}{s_r} c_{j\uparrow}^\dagger c_{j\downarrow}^\dagger c_{r\uparrow} c_{r\downarrow} \rangle = 0.25$ has the maximum value that

can be achieved by a product state. For arbitrary μ_H both values are independent of the system size N and site indexes j and r which means the state (III.8) has off-diagonal long-range order [59]. The state $|\psi_0^\eta\rangle$ (III.8) and its excitations are a linear combination of the states in the original tower (II.9).

We thus establish that the BCS wavefunction $|\psi_0^\eta\rangle$ is a linear combination of the eta-pairing states!

As shown in Appendix A 1 the Bogoliubov-transformed fermions diagonalizing

$$H_0^\eta = E \left[\left(\sum_j \gamma_{j1}^\dagger \gamma_{j1} - \gamma_{j2}^\dagger \gamma_{j2} \right) + 1 \right] \quad (\text{III.9})$$

are

$$\gamma_{j1}^\dagger = u c_{j\uparrow}^\dagger - s_j^* v^* c_{j\downarrow}; \quad \gamma_{j2}^\dagger = s_j^* v^* c_{j\uparrow} + u c_{j\downarrow}^\dagger \quad (\text{III.10})$$

Both operators γ_{j1} and γ_{j2} exactly annihilate the BCS ground state $|\psi_0^\eta\rangle$ (III.8). The raising operator $\mathcal{O}^{\eta\dagger}$ is constructed by replacing the original fermion operators with γ_j^\dagger in eq. (III.2)

$$\mathcal{O}^{\eta\dagger} = \frac{1}{2} \sum_j s_j \left(\gamma_{j1}^\dagger \gamma_{j2}^\dagger - \gamma_{j2}^\dagger \gamma_{j1}^\dagger \right). \quad (\text{III.11})$$

It coincides with the general expression (II.18) and creates the tower of excitations above the BCS ground state $|\psi_0^\eta\rangle$ (III.8) that forms the full transformed basis of the scar subspace (II.9).

C. Ground state for type-II ζ

For complex-valued hopping in (III.1) and $\mathcal{O}_j^\dagger = \zeta_j^\dagger = c_{j\uparrow}^\dagger c_{j\downarrow}$ the Hamiltonian governing the scar subspace is

$$H_0^\zeta = H_0^{H\zeta} + \delta H_0^\zeta. \quad (\text{III.12})$$

It is of the general form (II.11) with $\mu = 0$, $C = \mu_H N$. The lowest-energy state within the scar subspace (II.21) and the large- γ global ground state is given by

$$|\psi_0^\zeta\rangle = 2^{-\frac{N}{2}} \prod_j \left(1 + e^{i\theta} c_{j\uparrow}^\dagger c_{j\downarrow} \right) |0_{II}\rangle. \quad (\text{III.13})$$

In agreement with the general argument (II.29) its one- and two-point (ODLRO) functions are $\langle c_{j\uparrow}^\dagger c_{j\downarrow} \rangle = e^{-i\theta} 0.5$ and $\langle c_{j\uparrow}^\dagger c_{j\downarrow} c_{r\downarrow}^\dagger c_{r\uparrow} \rangle = e^{-i2\theta} 0.25$ and are independent of the system size N and of the positions where they are evaluated.

In Appendix A 2 we show that in terms of the emergent fermion operators

$$\gamma_{j1}^\dagger = u c_{j\uparrow}^\dagger - v^* c_{j\downarrow}^\dagger; \quad \gamma_{j2} = v^* c_{j\uparrow} + u c_{j\downarrow} \quad (\text{III.14})$$

H_0^ζ is simply the total "magnetization" with respect to the flavour of the transformed fermions

$$H_0^\zeta = \gamma \sum_j \gamma_{j1}^\dagger \gamma_{j1} - \gamma_{j2}^\dagger \gamma_{j2}. \quad (\text{III.15})$$

The raising operator creating scar excitations above $|\psi_0^\zeta\rangle$ (III.13) flips the "spin"/flavour of the transformed fermions analogous to ζ_j^\dagger (III.2).

$$O_j^{\gamma^\dagger} = \gamma_{j1}^\dagger \gamma_{j2}. \quad (\text{III.16})$$

D. Benefits of many-body scars

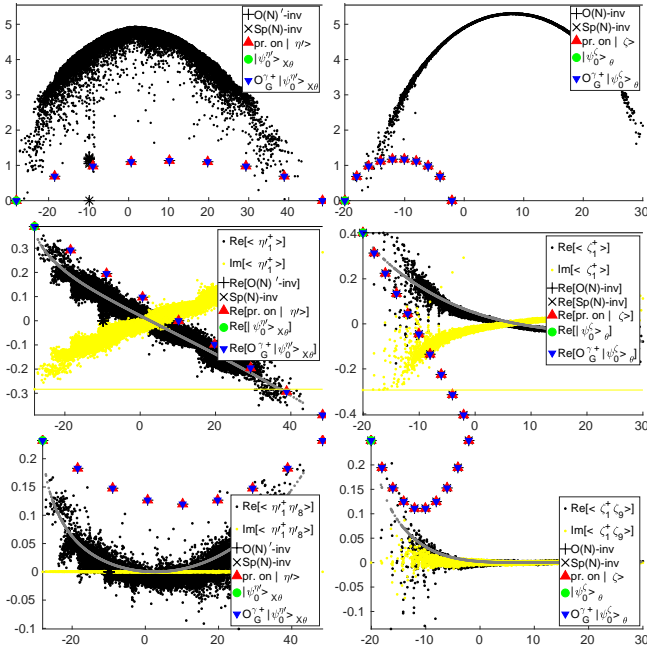


FIG. III.1. Numerical results for single-flavour ($K = 1$) 2D real-hopping Hubbard model with o.b.c., $U = 5.01$, $\mu = -1.2294$, $\theta = \pi/5$. $O^\dagger = \eta^\dagger$ in a),c),e) with $N_x \times N_y = 2 \times 4$ and $\gamma = 4.61$. $O^\dagger = \zeta^\dagger$ in b),d),f) with $N_x \times N_y = 3 \times 3$ and $\gamma = 1$ a),b) entanglement entropy c),d) one-point function $\langle O^\dagger \rangle_j$ on site (1,1). Black and yellow horizontal lines indicate the analytical prediction (II.29); e),f) two-point function (ODLRO) $\langle O_i^\dagger O_j \rangle$ where site i is (1,1) and site j is (N_x, N_y) . In a),c),e) the calculation is performed at fixed (even) total fermion number parity and in b),d),f) at fixed (half-filling) total particle number. Horizontal axis in all the plots is energy.

Because $|\psi_0\rangle$ and its O^{γ^\dagger} excitations are scar states the conclusions here hold for any deformed Hamiltonian

$$\tilde{H} = H^H + \delta H_0 + \sum_l O_l T_l, \quad (\text{III.17})$$

where O_l is an arbitrary operator and T_l is a generator of the symmetry group of one of the three scar families.

Ref. [2] provides an exhaustive list of such generators. They include arbitrary-range hopping terms, spin-orbit coupling (for the eta states $O_j = \eta_j$), magnetic field (for eta and eta') and many others. Furthermore the same Ref. [2] shows that many commonly used interactions such as Hubbard and Heisenberg also decompose as $H_0 + OT$. Thus such interactions might at most shift the values of μ and γ but usually only contribute OT terms that are irrelevant within the scar subspace.

We confirm our analytical conclusions by diagonalizing exactly numerically small 2D systems with the results for the eta' and zeta states shown in Fig. III.1 and for the eta states in the Appendix Fig. C.1. To illustrate the stability of our solution (III.17) we choose

$$\sum_l O_l T_l = \sum_{\langle i,j \rangle, p} T_{i,j} O_{ip} T_{i,j}, \quad (\text{III.18})$$

$$T_{i,j} = t \sum_{\sigma, p} c_{ip\sigma}^\dagger c_{jp\sigma} + h.c.,$$

$$O_{ip} = \left(r_{\sigma, \sigma'}^{(1)i,p} c_{ip\sigma}^\dagger c_{i(p+1)\sigma'} + r_{\sigma, \sigma'}^{(2)i,p} c_{ip\sigma}^\dagger c_{i(p+1)\sigma'} + h.c. \right)$$

with $r_{\sigma, \sigma'}^{(i)b,p}$ - real random numbers, uniformly distributed between 0 and 1. Here t is chosen to be the same as the amplitude of the hopping term. It is $t = e^{i\sqrt{2}\pi}$ for the zeta states and $t = 1$ for the eta' states. These additional terms are intended to simulate some quite drastic and strong perturbation that can be added to the Hubbard model without disturbing the BCS scar ground state and its excitations. We also choose it to be quite chaotic such that it breaks most symmetries of the full Hamiltonian.

Within the total fermion number parity (or half-filling for zeta states) sector the full Hamiltonian (III.17), indeed has no other symmetries remaining. The bulk of its spectrum (excluding scars) is fully ergodic with the level statistics parameter (average ratio of consecutive energy gaps [68]) $\langle r \rangle = 0.5325$ which is rather close to 0.5359 expected [68] in a generalized orthogonal ensemble (GOE, real, symmetric, random matrix). The ergodicity of the spectrum bulk is also confirmed by the energy gap distribution that follows the one expected for GOE and exhibits absence of near-zero gaps as a consequence of level repulsion. The data for $O = \eta$ is shown in Fig. C.1 d) and the results for $O = \eta'$ are identical.

The ground states ψ_0 (III.8) and (III.13) (green filled circles in Fig. III.1) and the excitations $(O^{\gamma^\dagger})^n |\psi_0\rangle$ above them (blue triangles) are identified by an exact identity overlap. In all the cases that we have studied numerically the ground state (II.9) has the largest (over the full Hilbert space) expectation value for both 1- $\langle O_j^\dagger \rangle$ and 2-point $\langle O_i^\dagger O_j \rangle$ function also at finite μ where we do not have an analytical argument guaranteeing this. Furthermore scars spanned by (II.9) have higher $\langle O_i^\dagger O_j \rangle$ (ODLRO) as a subspace. Indeed, the average absolute value of ODLRO over the eta' states (Fig. III.1 e)) is 12.5 times larger than the average value over the remaining states. Similarly for the zeta states this factor is

71! This shows that although adding the pairing potential δH_0 does induce the corresponding fluctuations in all the generic states, ODLRO in the scar subspace remains significantly larger.

Red triangles in Fig. III.1 indicate the states that fully lie within the subspace spanned by (II.9) with the original raising operator (III.2). Blue triangles indicate the states created by the transformed raising operators $\mathcal{O}_j^{\gamma\dagger}$ (eqs. (III.11) and (III.16)) above the respective ground states $|\psi_0^\eta\rangle$ and $|\psi_0^\zeta\rangle$. The fact that the two groups of states coincide confirms that these ground states and the "mean-field" excitations above them form a new basis in the original scar subspace (II.9). For the case of eta' states this confirms that the BCS wavefunction and its excitations are linear combinations of the eta-pairing states.

E. What γ is large enough?

At a relatively high $U = 8$ and low γ of about 0.69 the spectrum separates into the Mott "lobes" corresponding to fixed Hubbard-U energy that are broadened by the hopping and pairing potential as can be seen in Fig. C.2 a) and b). If Hubbard is repulsive the lobe containing the eta and eta' subspaces is highest in energy. Therefore to make the BCS wavefunction the ground state the value of γ roughly needs to exceed the bandwidth of all other Hamiltonian terms. In our numerical experiments with unity hopping amplitude the required γ_c is about the same as the Hubbard U . For attractive Hubbard the eta/eta' subspace is in the lowest energy "lobe" and to make BCS state the ground state γ_c only needs to exceed the bandwidth of that lobe. Numerically we observe that the required γ_c is about $U/10$. More detailed discussion of our numerical experiments can be found in Appendix C.2.

IV. EXAMPLE 2: INTER-ORBITAL MAGNETISM IN A TWO-ORBITAL GENERALIZED HUBBARD MODEL

Consider an example of the type-II Hilbert space with $K = 2$ orbitals or fermion flavours per site: A and B and the inter-orbital magnetic excitation creation operator

$$\mathcal{O}_j^\dagger = c_{j\uparrow}^{A\dagger} c_{j\downarrow}^B + c_{j\uparrow}^{B\dagger} c_{j\downarrow}^A \quad (\text{IV.1})$$

that couples the spin and orbital degrees of freedom.

We start from a generalized Hubbard Hamiltonian in external magnetic field B

$$H^B = B \sum_{i=1}^N (n_{i\uparrow} - n_{i\downarrow}) + \sum_{\langle kj \rangle} (t_{kj} c_j^\dagger c_k + h.c.) + U \sum_j H_j^{\zeta H_{ub}}, \quad (\text{IV.2})$$

where the hopping amplitudes t_{kj} are imaginary (and are thus generators of $O(N)$ [2]) and the generalized 2-orbital Hubbard interaction [67] $\sum_j H_j^{\zeta H_{ub}}$ with

$$H_j^{\zeta H_{ub}} = \frac{1}{2}(n_j^2 - n_j) = \frac{1}{2}n_j(n_j - 1), \quad (\text{IV.3})$$

is $O(N)$ -invariant and acts as a constant on any half-filled states including the scar subspace spanned by $|\phi_n\rangle$ (II.9) with \mathcal{O} from (IV.1). In the single-flavour ($K=1$) case this interaction is identical to the standard Hubbard interaction. In the present two-flavour case ($K=2$) it can also be written [67] as

$$H_j^{\zeta H_{ub}} = \sum_{\sigma} n_{jA\sigma} n_{jB\sigma} + \sum_p n_{jp\uparrow} n_{jp\downarrow} + \sum_{p,q} n_{jp\uparrow} \sigma_{pq}^1 n_{jq\downarrow}, \quad (\text{IV.4})$$

which is a special case of the on-site Coulomb interaction for Sr_2RuO_4 considered in [69].

The particle number operator is

$$n_j = n_{j\uparrow} + n_{j\downarrow} = \sum_{p=A}^B c_{j,\uparrow}^{p\dagger} c_{j,\uparrow}^p + \sum_{p=A}^B c_{j,\downarrow}^{p\dagger} c_{j,\downarrow}^p \quad (\text{IV.5})$$

The first and last terms of the Hamiltonian (IV.2) are $O(N)$ -invariant and therefore qualify [1] as H_0 with respect to the group $O(N)$. The H_0 part of the Hamiltonian upon addition of δH_0 (II.12) then reads

$$H_0^{ib\zeta} = B \sum_{i=1}^N (n_{i\uparrow} - n_{i\downarrow}) - \gamma \sum_j (e^{i\theta} \mathcal{O}_j^\dagger + e^{-i\theta} \mathcal{O}_j), \quad (\text{IV.6})$$

where we omitted the constant coming from the Hubbard interaction.

The second term in eq. (IV.2) is made of the generators of $O(N)$ and therefore exactly annihilates $O(N)$ -invariant states including the scar tower $|\phi_n\rangle$ (II.9).

Therefore the general solution from Sec. II C can be used identifying $\mu = B$. Thus the lowest energy scar state is given by

$$|\psi_g^{ib\zeta}\rangle = N_\psi \prod_j \left(1 + \frac{v}{u} \mathcal{O}_j^\dagger + \frac{(\frac{v}{u} \mathcal{O}_j^\dagger)^2}{2} \right) |0_\phi\rangle. \quad (\text{IV.7})$$

For the numerical calculations presented in Fig. IV.1 we again consider the Hamiltonian where a perturbation (III.18) with $t = i$ (that has no effect on the scar subspace) is added to the Hubbard model (IV.2)

$$H^{ib\zeta} = H^B + \delta H_0 + \sum_l O_l T_l, \quad (\text{IV.8})$$

Note that besides the actual inter-band zeta states $|\phi_n\rangle$ (II.9) we are interested in, a number of further $O(N)$

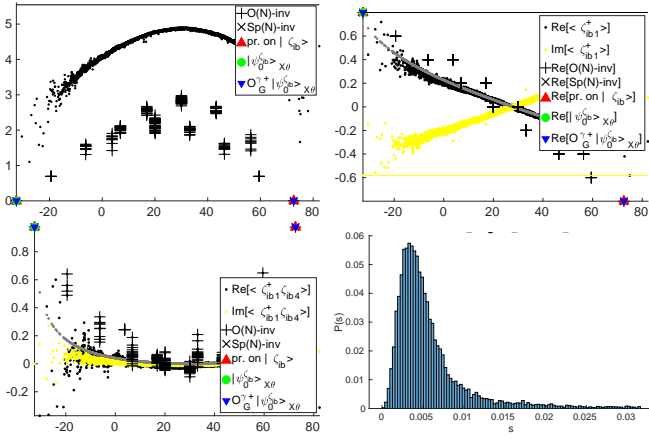


FIG. IV.1. Numerical exact diagonalization results for $K = 2$, inter-band zeta \mathcal{O} (IV.1) and the generalized Hubbard Hamiltonian (IV.8). One dimension, $N = 4$, $t = i$, $B = 1$, $U = 5.01$, $\gamma = 6.5$. Calculation is performed at fixed total particle number (half-filling). a) Entanglement entropy (middle cut) b) One-point function $\langle \mathcal{O}_j^\dagger \rangle$ at site $j = 1$ c) Two-point function (ODLRO) $\langle \mathcal{O}_i^\dagger \mathcal{O}_j \rangle$ with $i = 1$ and $j = N$. d) Distribution of the energy gaps in the full Hilbert space with the exception of the $O(N)$ -symmetric subspace. Horizontal axis in a), b), c) is energy.

symmetric scars are present for the model $H^{ib\zeta}$. Many of them for the Hamiltonian (IV.8) are degenerate with some of the excitations above the BCS scar ground state which prevents these from being identified as such numerically. In Appendix C3 and Fig. C.3 we show that additional Hamiltonian terms can be added to remove this degeneracy and make all the excitations clearly visible.

Using the type-II spinor basis and performing the Bogoliubov transformation (see Sec. A3) we find the new fermionic operators (with "orbital" index C, D and "spin" index 1,2)

$$\gamma_{j1}^{C\dagger} = u^* c_{j\uparrow}^{A\dagger} - v^* c_{j\downarrow}^{B\dagger} \quad (IV.9)$$

$$\gamma_{j1}^{D\dagger} = u^* c_{j\uparrow}^{B\dagger} - v^* c_{j\downarrow}^{A\dagger} \quad (IV.10)$$

$$\gamma_{j2}^C = v^* c_{j\uparrow}^A + u^* c_{j\downarrow}^B \quad (IV.11)$$

$$\gamma_{j2}^D = v^* c_{j\uparrow}^B + u^* c_{j\downarrow}^A \quad (IV.12)$$

$$(IV.13)$$

in terms of which the Hamiltonian $H^{ib\zeta}$ within the scar subspace is simply the total magnetization with respect to the "spin" of the transformed fermions

$$H_0^{ib\zeta} = E \sum_{p=C}^D (n_1^p - n_2^p) \quad (IV.14)$$

The raising operator (II.18) in the transformed tower that creates excitations above the ground state (IV.7)

coincides with the original raising operator (IV.1) written in terms of the Bogoliubov-transformed fermions

$$\mathcal{O}^{\dagger} = \sum_j \gamma_{j1}^{C\dagger} \gamma_{j2}^D + \gamma_{j1}^{D\dagger} \gamma_{j2}^C \quad (IV.15)$$

V. DISCUSSION AND OUTLOOK

The solution presented here does not materially depend on the matrices A (eq. (II.1)) and \tilde{A} (eq. (II.4)) that specify the particular type of pairing. Therefore our conclusions hold for any compatible type of pairing including unconventional! It would be interesting to see if our approach can be extended to pairing operators \mathcal{O}_j that act on more than one site.

Consider a strongly-interacting model such as Hubbard and decompose it as $H_0 + OT$. In many cases (as shown explicitly in the examples we considered) all the interactions are part of OT and annihilate the group-invariant scar subspace exactly or act on it as an irrelevant constant. Therefore, within the scar subspace, which is in some examples spanned by the BCS ground state and all its BCS excitations, all the dynamics is governed by H_0 only which coincides with the mean-field Hamiltonian. This presents an alternative view on the mean-field Hamiltonian as the exact Hamiltonian within the scar subspace rather than a rough approximation in the full Hilbert space.

Pure uniform mean-field BCS Hamiltonian (II.11) is $O(N)$ -invariant and can be regarded as H_0 . Its ground state is the BCS wavefunction which together with its excitations span the scar subspace. These states (and any dynamics within the scar subspace) remain identically unchanged for plenty of different OT terms (including interactions) added to the Hamiltonian which can be regarded as perturbations over the mean-field. For small strengths of these terms the BCS will remain the ground state (for higher strength and larger bandwidth of OT terms a non-scar may become lower in energy). Which means we show that the BCS wavefunction is a particularly stable solution even in presence of various OT interactions.

In Sec. IID we show that the state $|\psi_0\rangle$ has the maximum $\langle \mathcal{O}_i^\dagger \rangle$ over the full Hilbert space for $\mu = 0$. It therefore reacts the most to the term δH_0 (II.12). Let's say we have a Hamiltonian \tilde{H} of the form (II.10) that supports $O(N)$ -invariant scars but they are in the arbitrary positions in the spectrum. Adding to \tilde{H} a term $-\gamma(\mathcal{O}^\dagger + \mathcal{O})$ we will always, for large enough γ , obtain the ground state that is an $O(N)$ -invariant scar $|\psi_0\rangle$ (II.23). Because the terms \mathcal{O} are strictly local and relatively simple this provides the first practical protocol to initialize a fermionic system to a scar state in (a quantum simulator) experiment. For type-I the condition $\mu = \mu_H + U/2 = 0$ can be achieved by tuning the chemical potential μ_H using a global electric gate. For type-II by adjusting the

magnetic field. The term $\mathcal{O}^\dagger + \mathcal{O}$ may be induced by proximity or designed directly in a quantum simulator.

There exists (at least for fixed N) a critical value γ_c such that the ground state of the full system is in the scar subspace above it and in the remainder of the Hilbert space below. Suppose we start at $\gamma > \gamma_c$ and have a pure ground state that is fully located within the scar subspace. We now slowly lower γ staying at $T = 0$. A phase transition could be expected as we pass through γ_c . However, because of the ergodicity breaking and dynamical decoupling of the subspaces there are no matrix elements that could transform the wavefunction into the "would be" non-scar ground state beyond the transition. Instead the system will remain in a linear combination of scar states. Alternatively, from the same starting point we could keep γ fixed and start increasing the temperature. Because of the decoupling the state of the system can not leave the scar subspace and will turn into a linear combination of scars each of which has ODLRO $\langle \mathcal{O}_i^\dagger \mathcal{O}_j \rangle$ that is much larger than in generic states. It would be interesting to study how these predictions change if the Hamiltonian deviates [63] from the $H_0 + OT$ form.

Immediately after the eq. (II.23) we discuss the conditions for the higher-order clustering to dominate over the regular pairing in our general solution ground states. It would be interesting to investigate if this can be related to the so-called "4e-superconductivity" discussed in literature [70–76].

VI. ACKNOWLEDGEMENTS

We thank Manfred Sigrist for many illuminating discussions and acknowledge useful exchanges with Kirill Samokhin, Yuto Shibata and Ilaria Maccari. We also thank Igor Klebanov and Fedor Popov for the collaboration on the several related publications in preparation. The simulations presented in this work were performed on computational resources managed and supported by Princeton's Institute for Computational Science & Engineering and OIT Research Computing.

Appendix A: Solving the H_0 Hamiltonian using the Bogoliubov transformation

The H_0 Hamiltonian governing the scar subspace in the examples considered in Sections III and IV in the main text can alternatively be solved using a canonical transformation as is customary for the BCS mean field Hamiltonians.

1. Single-orbital: Eta subspace

With respect to the symmetry groups of the $|\eta\rangle$ and $|\eta'\rangle$ states the H_0 part of the Hamiltonian is given by eq. (III.7)

Let's write it (consider the case of eta states with $\mathcal{O}^\dagger = \eta_j^\dagger = c_{j\uparrow}^\dagger c_{j\downarrow}^\dagger$) using the type-I spinor (II.25) and $\mu = (U/2 + \mu_H)$

$$H_0^\eta = \sum_j \begin{pmatrix} c_{j\uparrow}^\dagger & c_{j\downarrow} \end{pmatrix} \begin{pmatrix} \mu & -\gamma e^{i\theta} \\ -\gamma e^{-i\theta} & -\mu \end{pmatrix} \begin{pmatrix} c_{j\uparrow} \\ c_{j\downarrow}^\dagger \end{pmatrix} + \mu N \quad (\text{A.1})$$

Observe that this Hamiltonian is very similar to the BCS mean-field Hamiltonian [3]

$$H_0 = \sum_k \begin{pmatrix} c_{k\uparrow}^\dagger & c_{-k\downarrow} \end{pmatrix} \begin{pmatrix} \xi_k & -\Delta_k \\ -\Delta_k^* & -\xi_k \end{pmatrix} \begin{pmatrix} c_{k\uparrow} \\ c_{-k\downarrow}^\dagger \end{pmatrix} + K_0 \quad (\text{A.2})$$

We can therefore diagonalize (A.1) using the Bogoliubov canonical transformation.

$$H_0 = \sum_j E_1 \gamma_{j1}^\dagger \gamma_{j1} + E_2 \gamma_{j2}^\dagger \gamma_{j2} - E_2 = \quad (\text{A.3})$$

$$\begin{pmatrix} \gamma_{j1}^\dagger & \gamma_{j2} \end{pmatrix} \begin{pmatrix} E_1 & 0 \\ 0 & E_2 \end{pmatrix} \begin{pmatrix} \gamma_{j1} \\ \gamma_{j2}^\dagger \end{pmatrix} - E_2 \quad (\text{A.4})$$

Where

$$\begin{pmatrix} c_{j\uparrow} \\ c_{j\downarrow}^\dagger \end{pmatrix} = U_j \begin{pmatrix} \gamma_{j1} \\ \gamma_{j2}^\dagger \end{pmatrix}, \quad (\text{A.5})$$

$$U_j = \begin{pmatrix} u_j^* & v_j \\ -v_j^* & u_j \end{pmatrix}, \quad (\text{A.6})$$

$E_1 = -E_2 = E$ and the definitions of eq. (II.22) are used.

The creation operators of the new emergent fermions are given in eq. (III.10).

The eigenstates of (A.3) is a tower of $N + 1$ states (II.9) with the raising operator that creates one additional quasiparticle of each type

$$\mathcal{O}_j^{\gamma\dagger} = \gamma_{j1}^\dagger \gamma_{j2}^\dagger \quad (\text{A.7})$$

The lowest-energy state $|\psi_0^\eta\rangle$ in the tower scar subspace (III.8), the BCS wavefunction, has no excitations of either type and thus satisfies for any site j

$$\mathcal{O}_j^\gamma |\psi_0^\eta\rangle = 0 \quad (\text{A.8})$$

2. Single-orbital: Zeta subspace

With respect to the symmetry group of the $|\zeta\rangle$ states the H_0 part of the Hamiltonian is given by eq. (III.12).

Using the type-II spinor (II.26) we write it as

$$H_0^\zeta = \sum_j \begin{pmatrix} c_{j\uparrow}^\dagger & c_{j\downarrow}^\dagger \end{pmatrix} \begin{pmatrix} 0 & -\gamma e^{i\theta} \\ -\gamma e^{-i\theta} & 0 \end{pmatrix} \begin{pmatrix} c_{j\uparrow} \\ c_{j\downarrow} \end{pmatrix} + \mu N \quad (\text{A.9})$$

The transformation is the same as in the eta case (replacing $\mu = 0$ and using definitions (A.6), (II.22))

$$\begin{pmatrix} c_{j\uparrow} \\ c_{j\downarrow} \end{pmatrix} = U_j \begin{pmatrix} \gamma_{j1} \\ \gamma_{j2} \end{pmatrix} \quad (\text{A.10})$$

leading to the new fermion operators given in eq. (III.14).

The Hamiltonian after the canonical transformation is

$$H_0^\zeta = \begin{pmatrix} \gamma_{j1}^\dagger & \gamma_{j2}^\dagger \end{pmatrix} \begin{pmatrix} E_1 & 0 \\ 0 & E_2 \end{pmatrix} \begin{pmatrix} \gamma_{j1} \\ \gamma_{j2} \end{pmatrix} = E \sum_j \gamma_{j1}^\dagger \gamma_{j1} - \gamma_{j2}^\dagger \gamma_{j2} \quad (\text{A.11})$$

and is the total "magnetization" wrt to the flavour of the transformed fermions.

The eigenstates of (A.11) is a tower of states (II.9) where the raising operator is (III.16). The lowest energy state (III.13) in the tower has the BCS form.

3. Two-orbital: Inter-band zeta

In the type-II spinor (II.26) basis the H_0 part of the Hamiltonian relevant for the scar subspace reads

$$\begin{pmatrix} c_{j\uparrow}^{A\dagger} & c_{j\uparrow}^{B\dagger} & c_{j\downarrow}^{A\dagger} & c_{j\downarrow}^{B\dagger} \end{pmatrix} \begin{pmatrix} B & 0 & 0 & -\gamma e^{i\theta} \\ 0 & B & -\gamma e^{i\theta} & 0 \\ 0 & -\gamma e^{-i\theta} & -B & 0 \\ -\gamma e^{-i\theta} & 0 & 0 & -B \end{pmatrix} \begin{pmatrix} c_{j\uparrow}^A \\ c_{j\uparrow}^B \\ c_{j\downarrow}^A \\ c_{j\downarrow}^B \end{pmatrix} \quad (\text{A.12})$$

it is diagonalized by the following unitary transformation

$$U = \begin{pmatrix} u^* & 0 & v & 0 \\ 0 & u^* & 0 & v \\ 0 & -v^* & 0 & u \\ -v^* & 0 & u & 0 \end{pmatrix} \quad (\text{A.13})$$

where u and v are given by (II.22) with $\mu = B$.

Appendix B: On the SU(2) generators forming the "basis" for eligible H_0 terms

Consider the $NK+1$ dimensional subspace of the scars spanned by the tower $|\phi_n\rangle$ (II.9).

Within this subspace and in this basis any valid H_0 Hamiltonian is given by a $(NK+1) \times (NK+1)$ matrix. Diagonal entries can only come from the commutator $[\mathcal{O}, \mathcal{O}^\dagger]$ which are chemical potential/magnetization terms. Let us introduce the restriction that for type-I all the chemical potential terms $\mu_\alpha n_\alpha$ must have the same

strength with μ thus independent of flavour α . Similarly, for type-II we require that all the couplings in the terms of the form $B_\alpha(n_{\alpha\uparrow} - n_{\alpha\downarrow})$ are the same with B independent of α .

The terms above and below diagonal come from \mathcal{O} and \mathcal{O}^\dagger respectively. Any other matrix element would connect $|n\rangle$ with $|m\rangle$ where $|m-n| \geq 2$. Which means such a matrix element can only be created by a Hamiltonian term that creates two or more excitations: $(\mathcal{O}^\dagger)^p$ with $p \geq 2$. Any such operator would need to be at least 4-body, such as $c^\dagger c^\dagger \dots c^\dagger$, multiplied $p \geq 4$ times. If we exclude those (unphysical and non-local) operators then any valid $O(N)$ -invariant H_0 within the scar subspace expands as a linear combination of the 3 SU(2) generators: $[\mathcal{O}, \mathcal{O}^\dagger]$, \mathcal{O} and \mathcal{O}^\dagger .

Appendix C: Additional numerical data

1. 2D single-orbital Hubbard model: eta scar subspace

In Fig. C.1 we present the numerical results for the 2D Hubbard model that are in many ways analogous to the ones presented in Fig. III.1 a),c),e) with the only major difference that $\mathcal{O}^\dagger = \eta^\dagger$ (III.2) was used here (instead of $\eta^{\dagger'}$) and the hopping in the Hamiltonian (III.17) is purely imaginary (instead of purely real).

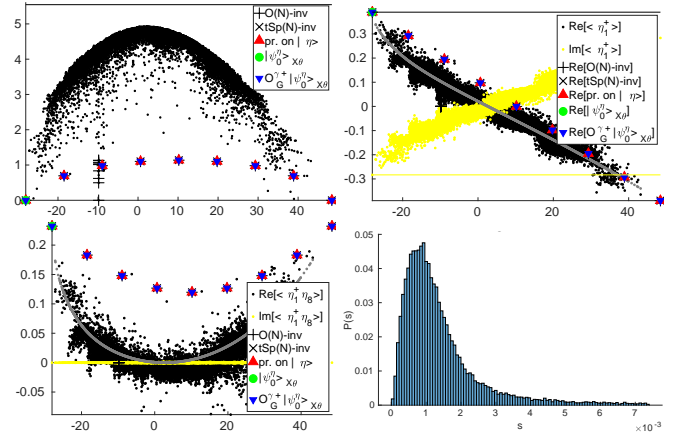


FIG. C.1. Numerical results for o.b.c., $U = 5.01$, $\mu = -1.2294$, $\theta = \pi/5$. with $N_x \times N_y = 2 \times 4$ and $\gamma = 4.61$. a) entanglement entropy (cut separates the "top" 5 sites (two top rows without 1 site) from the remaining 4 sites (bottom row + 1 site)) b) one-point function $\langle \mathcal{O}^\dagger \rangle_j$ on site (1,1), c) two-point function (ODLRO) $\langle \mathcal{O}_i^\dagger \mathcal{O}_j \rangle$ where site i is (1,1) and site j is (N_x, N_y) . d) Energy gap histogram. Horizontal axis in a),b),c) is energy. The calculation is performed at fixed (even) total fermion number parity.

2. 2D single-orbital Hubbard model: position of the eta and eta' scars in spectrum for $\mu = 0$

At a relatively high $U = 8$ and low $\gamma = 0.69$ the spectrum separates into the Mott "lobes" corresponding to fixed Hubbard- U energy that are broadened by the hopping and pairing potential as can be seen in Fig. C.2 a) and b). If Hubbard is repulsive ($U > 0$, Fig. C.2 a) the lobe containing the eta subspace is highest in energy because the eta pairing states contain pairs of opposite spins on the same site which has high Hubbard- U cost. To make the state $|\psi_0^{\eta'}\rangle$ the g.s. in a repulsive Hubbard model a relatively high $\gamma = 6.9$ is needed, see Fig. C.2 c) as the splitting induced by γ needs to extend beyond the bandwidth of the rest of the Hamiltonian. Note that the lobes observed in Fig. C.2 c) are due to the γ term now, not U , so γ actually dominates the spectrum there.

For the attractive Hubbard ($U < 0$) the U -lobes are flipped and the eta subspace is in the lowest-energy lobe, see Fig. C.2 b). Now to make the state $|\psi_0^{\eta'}\rangle$ to be the g.s. the splitting induced by γ only needs to exceed the "bandwidth" of this one lobe (the energy scale should be given by the hopping amplitude). For the parameters considered the required $\gamma = 0.69$ is 10 times smaller than the threshold for the repulsive Hubbard.

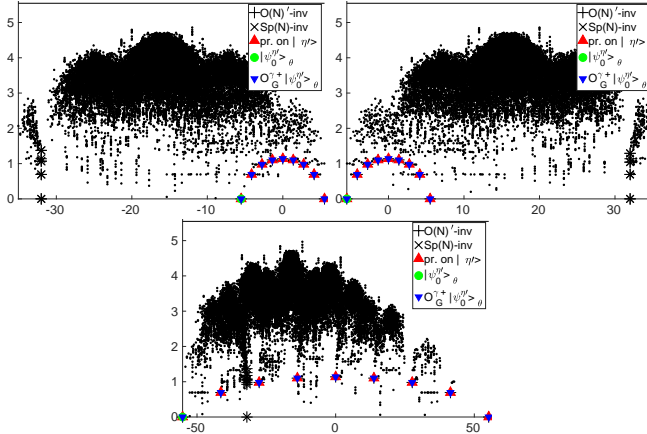


FIG. C.2. $N=6$. obc., $t=1$, real-hopping Hubbard model. $\theta = \pi/5$. entanglement entropy a) $\gamma = 0.69$, $U=8$, $\mu = -4$, repulsive Hubbard b) $\gamma = 0.69$, $U=-8$, $\mu_H = 4$, attractive Hubbard c) $\gamma = 6.9$, $U=8$, $\mu_H = -4$, repulsive Hubbard. TOT term that we usually use with scars is turned off so the Hamiltonian is purely Hubbard. Horizontal axis is energy.

3. Two-orbital inter-band magnetism

The H_0 of the Hamiltonian (IV.8) leaves some of the states in the inter-band zeta subspace degenerate with

other $O(N)$ singlets which leads to the eigenvectors we obtain having mixed character and being not identifiable as can be seen in Fig. IV.1 where only the BCS-like ground state and the highest excitation in the tower are found by overlap.

To lift the degeneracy we add here the following terms to the Hamiltonian (IV.8): quadratic Casimir of the group $Sp(2N)$, quadratic Casimir of the group $Sp(N)$ and the spin-orbit coupling from Ref. [69]

$$H_{SO} = -\lambda i \sum_{r\alpha\beta} \sigma_{\alpha\beta}^z c_{rA\alpha}^\dagger c_{rB\beta} + \text{H.c.} \quad (\text{C.1})$$

The inter-band zeta states have at least $Sp(N)$ symmetry (which includes $O(N)$ as a subgroup). They also have a fixed representation of $Sp(2N)$ group. This is why the mentioned terms become part of H_0 . Once the full symmetry group of these states is known it will be possible to replace the long-range Casimir terms with other short-range generators.

Fig. C.3 confirms that once the unwanted degeneracies are lifted all the $2N = 8$ excitations (blue triangles) above the BCS-like ground state can be exactly identified in agreement with the general solution.

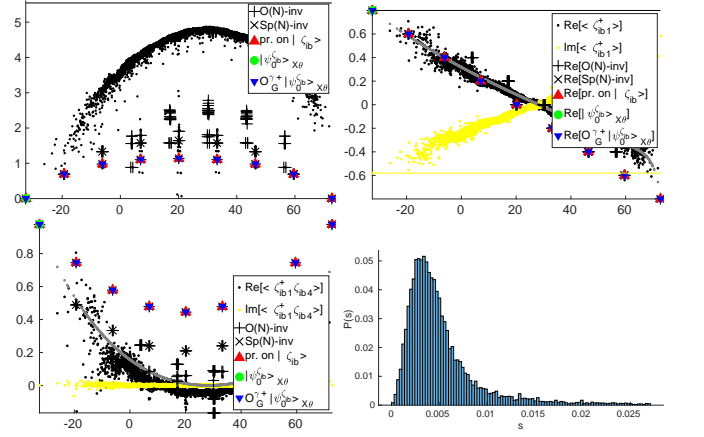


FIG. C.3. Numerical calculation for the inter-band zeta \mathcal{O} (IV.1) and additional terms added to (IV.8). Another difference is that here complex hopping amplitude is used as opposed to the imaginary one in (IV.8). 1D, $K = 2$, $N = 4$, $B = 1$, $U = 5.01$, $\gamma = 6.5$. a) Entanglement entropy b) $\langle \mathcal{O}_1^\dagger \rangle$ c) $\langle \mathcal{O}_4^\dagger \rangle$ d) Histogram of the energy gaps with $O(N)$ singlets excluded from the spectrum. Horizontal axis in a), b), c) is energy. Calculation is performed at fixed total particle number (half-filling).

- [1] K. Pakrouski, P. N. Pallegar, F. K. Popov, and I. R. Klebanov, Many-body scars as a group invariant sector of hilbert space, *Phys. Rev. Lett.* **125**, 230602 (2020).
- [2] K. Pakrouski, P. N. Pallegar, F. K. Popov, and I. R. Klebanov, Group theoretic approach to many-body scar states in fermionic lattice models, *Phys. Rev. Res.* **3**, 043156 (2021), [arXiv:2106.10300 \[cond-mat.str-el\]](https://arxiv.org/abs/2106.10300).
- [3] M. Tinkham, Introduction to Superconductivity (McGraw-Hill, 1996).
- [4] H. Bernien, S. Schwartz, A. Keesling, H. Levine, A. Omran, H. Pichler, S. Choi, A. S. Zibrov, M. Endres, M. Greiner, V. Vuletić, and M. D. Lukin, Probing many-body dynamics on a 51-atom quantum simulator, *Nature* **551**, 579 EP (2017).
- [5] M. Serbyn, D. A. Abanin, and Z. Papić, Quantum many-body scars and weak breaking of ergodicity, *Nature Physics* **10.1038/s41567-021-01230-2** (2021).
- [6] S. Moudgalya, B. A. Bernevig, and N. Regnault, Quantum many-body scars and hilbert space fragmentation: a review of exact results, *Reports on Progress in Physics* **85**, 086501 (2022).
- [7] Z. Papić, Weak ergodicity breaking through the lens of quantum entanglement, in *Entanglement in Spin Chains: From Theory to Quantum Technology Applications*, edited by A. Bayat, S. Bose, and H. Johannesson (Springer International Publishing, Cham, 2022) pp. 341–395.
- [8] A. Chandran, T. Iadecola, V. Khemani, and R. Moessner, Quantum many-body scars: A quasiparticle perspective, *Annual Review of Condensed Matter Physics* **14**, 443 (2023), <https://doi.org/10.1146/annurev-conmatphys-031620-101617>.
- [9] I. Lesanovsky and H. Katsura, Interacting fibonacci anyons in a rydberg gas, *Phys. Rev. A* **86**, 041601(R) (2012).
- [10] N. Shiraishi and T. Mori, Systematic construction of counterexamples to the eigenstate thermalization hypothesis, *Phys. Rev. Lett.* **119**, 030601 (2017).
- [11] C. J. Turner, A. A. Michailidis, D. A. Abanin, M. Serbyn, and Z. Papić, Weak ergodicity breaking from quantum many-body scars, *Nature Physics* **14**, 745 (2018).
- [12] S. Moudgalya, N. Regnault, and B. A. Bernevig, Entanglement of exact excited states of affleck-kennedy-lieb-tasaki models: Exact results, many-body scars, and violation of the strong eigenstate thermalization hypothesis, *Phys. Rev. B* **98**, 235156 (2018).
- [13] S. Choi, C. J. Turner, H. Pichler, W. W. Ho, A. A. Michailidis, Z. Papić, M. Serbyn, M. D. Lukin, and D. A. Abanin, Emergent SU(2) Dynamics and Perfect Quantum Many-Body Scars, *Phys. Rev. Lett.* **122**, 220603 (2019).
- [14] V. Khemani, M. Hermele, and R. Nandkishore, Localization from hilbert space shattering: From theory to physical realizations, *Phys. Rev. B* **101**, 174204 (2020).
- [15] P. Sala, T. Rakovszky, R. Verresen, M. Knap, and F. Pollmann, Ergodicity breaking arising from hilbert space fragmentation in dipole-conserving hamiltonians, *Phys. Rev. X* **10**, 011047 (2020).
- [16] S. Moudgalya, A. Prem, R. Nandkishore, N. Regnault, and B. A. Bernevig, Thermalization and its absence within krylov subspaces of a constrained hamiltonian, (2019), [arXiv:1910.14048 \[cond-mat.str-el\]](https://arxiv.org/abs/1910.14048).
- [17] M. Schecter and T. Iadecola, Weak ergodicity breaking and quantum many-body scars in spin-1 xy magnets, *Phys. Rev. Lett.* **123**, 147201 (2019).
- [18] B. Buča, J. Tindall, and D. Jaksch, Non-stationary coherent quantum many-body dynamics through dissipation, *Nature Communications* **10**, 1730 (2019).
- [19] O. Vafek, N. Regnault, and B. A. Bernevig, Entanglement of Exact Excited Eigenstates of the Hubbard Model in Arbitrary Dimension, *SciPost Phys.* **3**, 043 (2017).
- [20] T. Iadecola and M. Žnidarič, Exact localized and ballistic eigenstates in disordered chaotic spin ladders and the fermi-hubbard model, *Phys. Rev. Lett.* **123**, 036403 (2019).
- [21] N. Shibata, N. Yoshioka, and H. Katsura, Onsager’s Scars in Disordered Spin Chains, *Phys. Rev. Lett.* **124**, 180604 (2020), [arXiv:1912.13399 \[quant-ph\]](https://arxiv.org/abs/1912.13399).
- [22] A. A. Michailidis, C. J. Turner, Z. Papić, D. A. Abanin, and M. Serbyn, Stabilizing two-dimensional quantum scars by deformation and synchronization, *Phys. Rev. Res.* **2**, 022065(R) (2020).
- [23] D. K. Mark and O. I. Motrunich, η -pairing states as true scars in an extended hubbard model, *Phys. Rev. B* **102**, 075132 (2020).
- [24] K. Bull, I. Martin, and Z. Papić, Systematic construction of scarred many-body dynamics in 1d lattice models, *Phys. Rev. Lett.* **123**, 030601 (2019).
- [25] V. Khemani, C. R. Laumann, and A. Chandran, Signatures of integrability in the dynamics of Rydberg-blockaded chains, *Phys. Rev. B* **99**, 161101(R) (2019).
- [26] K. Lee, R. Melendrez, A. Pal, and H. J. Changlani, Exact three-colored quantum scars from geometric frustration, *Physical Review B* **101**, 241111(R) (2020).
- [27] D. K. Mark, C.-J. Lin, and O. I. Motrunich, Unified structure for exact towers of scar states in the affleck-kennedy-lieb-tasaki and other models, *Phys. Rev. B* **101**, 195131 (2020).
- [28] T. Iadecola and M. Schecter, Quantum many-body scar states with emergent kinetic constraints and finite-entanglement revivals, *Physical Review B* **101**, 024306 (2020).
- [29] S. Moudgalya, N. Regnault, and B. A. Bernevig, η -pairing in hubbard models: From spectrum generating algebras to quantum many-body scars, *Phys. Rev. B* **102**, 085140 (2020).
- [30] B. van Voorden, J. c. v. Minář, and K. Schoutens, Quantum many-body scars in transverse field ising ladders and beyond, *Phys. Rev. B* **101**, 220305(R) (2020).
- [31] J. Ren, C. Liang, and C. Fang, Quasisymmetry groups and many-body scar dynamics, *Phys. Rev. Lett.* **126**, 120604 (2021).
- [32] N. O’Dea, F. Burnell, A. Chandran, and V. Khemani, From tunnels to towers: Quantum scars from lie algebras and q -deformed lie algebras, *Phys. Rev. Research* **2**, 043305 (2020).
- [33] N. S. Srivatsa, J. Wildeboer, A. Seidel, and A. E. B. Nielsen, Quantum many-body scars with chiral topological order in two dimensions and critical properties in one dimension, *Phys. Rev. B* **102**, 235106 (2020).
- [34] C.-J. Lin, V. Calvera, and T. H. Hsieh, Quantum many-body scar states in two-dimensional rydberg atom arrays, *Phys. Rev. B* **101**, 220304(R) (2020).
- [35] S. Moudgalya, E. O’Brien, B. A. Bernevig, P. Fendley, and N. Regnault, Large classes of quantum scarred hamiltonians from matrix product states, *Phys. Rev. B* **102**, 085120 (2020).

- (2020).
- [36] K. Mizuta, K. Takasan, and N. Kawakami, Exact floquet quantum many-body scars under rydberg blockade, *Phys. Rev. Research* **2**, 033284 (2020).
- [37] K. Bull, J.-Y. Desaulles, and Z. Papić, Quantum scars as embeddings of weakly broken lie algebra representations, *Phys. Rev. B* **101**, 165139 (2020).
- [38] Y. Kuno, T. Mizoguchi, and Y. Hatsugai, Multiple quantum scar states and emergent slow thermalization in a flat-band system, *Phys. Rev. B* **104**, 085130 (2021).
- [39] D. Banerjee and A. Sen, Quantum scars from zero modes in an abelian lattice gauge theory on ladders, *Phys. Rev. Lett.* **126**, 220601 (2021).
- [40] S. Pilatowsky-Cameo, D. Villaseñor, M. A. Bastarrachea-Magnani, S. Lerma-Hernández, L. F. Santos, and J. G. Hirsch, Ubiquitous quantum scarring does not prevent ergodicity, *Nature Communications* **12**, 852 (2021).
- [41] N. Maskara, A. A. Michailidis, W. W. Ho, D. Bluvstein, S. Choi, M. D. Lukin, and M. Serbyn, Discrete time-crystalline order enabled by quantum many-body scars: Entanglement steering via periodic driving, *Phys. Rev. Lett.* **127**, 090602 (2021).
- [42] C. M. Langlett, Z.-C. Yang, J. Wildeboer, A. V. Gorshkov, T. Iadecola, and S. Xu, Rainbow scars: From area to volume law, *Phys. Rev. B* **105**, L060301 (2022).
- [43] J. Ren, C. Liang, and C. Fang, Deformed symmetry structures and quantum many-body scar subspaces, *Phys. Rev. Res.* **4**, 013155 (2022).
- [44] L.-H. Tang, N. O’Dea, and A. Chandran, Multimagnon quantum many-body scars from tensor operators, *Phys. Rev. Res.* **4**, 043006 (2022).
- [45] F. Schindler, N. Regnault, and B. A. Bernevig, Exact quantum scars in the chiral nonlinear luttinger liquid, *Phys. Rev. B* **105**, 035146 (2022).
- [46] M. Dodelson and A. Zhiboedov, Gravitational orbits, double-twist mirage, and many-body scars, *Journal of High Energy Physics* **2022**, 163 (2022).
- [47] D. Liska, V. Gritsev, W. Vleeshouwers, and J. Minář, Holographic quantum scars, *SciPost Phys.* **15**, 106 (2023).
- [48] J.-Y. Desaulles, D. Banerjee, A. Hudomal, Z. Papić, A. Sen, and J. C. Halimeh, Weak ergodicity breaking in the schwinger model, *Phys. Rev. B* **107**, L201105 (2023).
- [49] J.-Y. Desaulles, A. Hudomal, D. Banerjee, A. Sen, Z. Papić, and J. C. Halimeh, Prominent quantum many-body scars in a truncated schwinger model, *Phys. Rev. B* **107**, 205112 (2023).
- [50] T. Budde, M. K. Marinković, and J. C. P. Barros, Quantum many-body scars for arbitrary integer spin in 2+1d abelian gauge theories (2024), arXiv:2403.08892 [hep-lat].
- [51] M. Iversen, J. H. Bardarson, and A. E. B. Nielsen, Tower of two-dimensional scar states in a localized system, *Phys. Rev. A* **109**, 023310 (2024).
- [52] R. Shen, F. Qin, J.-Y. Desaulles, Z. Papić, and C. H. Lee, Enhanced many-body quantum scars from the non-hermitian fock skin effect (2024), arXiv:2403.02395 [cond-mat.quant-gas].
- [53] J. Osborne, I. P. McCulloch, and J. C. Halimeh, Quantum many-body scarring in 2 + 1d gauge theories with dynamical matter (2024), arXiv:2403.08858 [cond-mat.quant-gas].
- [54] S. Moudgalya and O. I. Motrunich, Exhaustive Characterization of Quantum Many-Body Scars using Commutant Algebras, (2022), arXiv:2209.03377 [cond-mat.str-el].
- [55] J. de Boer, V. E. Korepin, and A. Schadschneider, η pairing as a mechanism of superconductivity in models of strongly correlated electrons, *Phys. Rev. Lett.* **74**, 789 (1995).
- [56] T. Kaneko, T. Shirakawa, S. Sorella, and S. Yunoki, Photoinduced η pairing in the hubbard model, *Phys. Rev. Lett.* **122**, 077002 (2019).
- [57] K. Gillmeister, D. Golež, C.-T. Chiang, N. Bittner, Y. Pavlyukh, J. Berakdar, P. Werner, and W. Widdra, Ultrafast coupled charge and spin dynamics in strongly correlated nio, *Nature Communications* **11**, 4095 (2020).
- [58] L. Gotta, L. Mazza, P. Simon, and G. Roux, Exact many-body scars based on pairs or multimers in a chain of spinless fermions, *Phys. Rev. B* **106**, 235147 (2022).
- [59] C. N. Yang, η pairing and off-diagonal long-range order in a hubbard model, *Phys. Rev. Lett.* **63**, 2144 (1989).
- [60] M. Nakagawa, H. Katsura, and M. Ueda, Exact eigenstates of multicomponent hubbard models: $Su(n)$ magnetic η pairing, weak ergodicity breaking, and partial integrability (2022), arXiv:2205.07235 [cond-mat.str-el].
- [61] C. N. Yang and S. Zhang, $So(4)$ symmetry in a hubbard model, *Modern Physics Letters B* **4**, 759 (1990).
- [62] S. Imai and N. Tsuji, Quantum many-body scars with unconventional superconducting pairing symmetries via multi-body interactions (2024), arXiv:2404.02914 [cond-mat.supr-con].
- [63] P. Kolb and K. Pakrouski, Stability of the many-body scars in fermionic spin-1/2 models, *PRX Quantum* **4**, 040348 (2023).
- [64] Z. Sun, F. K. Popov, I. R. Klebanov, and K. Pakrouski, Majorana scars as group singlets, *Phys. Rev. Res.* **5**, 043208 (2023).
- [65] Y. Nambu, Quasi-particles and gauge invariance in the theory of superconductivity, *Phys. Rev.* **117**, 648 (1960).
- [66] Z. Sun, F. K. Popov, I. R. Klebanov, and K. Pakrouski, Group structure of the hilbert space of multi-band, spin-1/2 lattice fermionic models (), in preparation.
- [67] Z. Sun, F. K. Popov, I. R. Klebanov, and K. Pakrouski, Toolbox for making multi-band fermionic scarred hamiltonians (), in preparation.
- [68] Y. Y. Atas, E. Bogomolny, O. Giraud, and G. Roux, Distribution of the ratio of consecutive level spacings in random matrix ensembles, *Phys. Rev. Lett.* **110**, 084101 (2013).
- [69] B. Zinkl and M. Sigrist, Impurity-induced magnetic ordering in sr_2RuO_4 , *Phys. Rev. Res.* **3**, 023067 (2021).
- [70] G. Röpke, A. Schnell, P. Schuck, and P. Nozières, Four-particle condensate in strongly coupled fermion systems, *Phys. Rev. Lett.* **80**, 3177 (1998).
- [71] E. Babaev, A. Sudbø, and N. W. Ashcroft, A superconductor to superfluid phase transition in liquid metallic hydrogen, *Nature* **431**, 666 (2004).
- [72] D. F. Agterberg and H. Tsunetsugu, Dislocations and vortices in pair-density-wave superconductors, *Nature Physics* **4**, 639 (2008).
- [73] E. Berg, E. Fradkin, and S. A. Kivelson, Charge-4e superconductivity from pair-density-wave order in certain high-temperature superconductors, *Nature Physics* **5**, 830 (2009).
- [74] M. O. Soldini, M. H. Fischer, and T. Neupert, Charge-4e superconductivity in a hubbard model, *Phys. Rev. B* **109**, 214509 (2024).
- [75] N. V. Gnezdilov and Y. Wang, Solvable model for a charge-4e superconductor, *Phys. Rev. B* **106**, 094508 (2022).
- [76] P. Li, K. Jiang, and J. Hu, Charge 4e superconductor: A wavefunction approach, *Science Bulletin* **69**, 2328 (2024).